Numerical Modeling of Shock-Wave Structures in Supersonic Flows of Non-Equilibrium Vibrationally Excited Gas

© S.S. Khrapov, A.V. Khoperskov, N.S. Khrapov

Volgograd State University,
Volgograd, Russia
e-mail: khrapov@volsu.ru

Received May 6, 2025
Revised June 10, 2025
Accepted June 10, 2025

The dynamics of two-dimensional flows of nonequilibrium gas is considered taking into account relaxation processes, viscosity and thermal conductivity. Based on the numerical gas-dynamic method MUSCL, a parallel computing algorithm is implemented, which allows studying nonlinear wave structures arising in a non-equilibrium medium due to the development of gas-dynamic instabilities with high spatial resolution. A significant increase (by 100−1000 times) in computing performance is shown when using parallel versions of the computing code for GPUs. Numerical modeling of shock-wave structures in a flat two-dimensional channel with injection of a supersonic jet of non-equilibrium gas is carried out.

Keywords: non-equilibrium gas, supersonic jets, shock waves, numerical methods, parallel computing on GPUs.

DOI: 10.61011/TP.2025.12.62477.247-25

Introduction

Supersonic non-equilibrium gas-dynamic flows can occur in nozzles of jet engines [1,2] during hypersonic flow around aerodynamic surfaces [3,4]. Nonequilibrium of a medium is induced by a difference of static and vibrational temperatures in a gas [5]. Due to various physical processes (electrical and VHF discharges, shockwaves during hypersonic flow, fast cooling of the supersonic jets), the vibrational gas temperature related to vibrational energy levels of polyatomic molecules can exceed the static gas temperature in several times [4,6,7]. In this case, relaxation processes start significantly affecting dynamics and a structure of the gas-dynamic flows [8–12]. At certain conditions, the non-equilibrium vibrationally-excited gas can become acoustically active and at a nonlinear stage of evolution of acoustic and thermal instabilities it can form variously-structured shockwaves (SW) [10,11]: a sawtooth system of weak shockwaves and a quasi-steady-state system of shock-wave pulses (SWP).

An important factor during numerical modeling of the non-equilibrium gas-dynamic flows with high spatial resolution is computational code performance, which affects both a result obtaining time as well as completeness of numerical solutions during mass calculations with various values of model parameters [13,14].

The present study is aimed at developing and testing an effective computational tool with high spatial resolution and accuracy for studying nonlinear wave structures that are formed in supersonic non-equilibrium flows of the vibrationally-excited gases at the various stages of evolution of gas-dynamic instabilities (an acoustic, thermal, of a tangential velocity break, corrugated instability of the shockwave). The two-dimensional numerical model was developed using a gas-dynamic modeling method MUSCL (Monotone Upwind Scheme for Conservation Laws) [15] that was adapted for integrating two-dimensional equations of non-equilibrium gas dynamics [10,11]. A parallel code of the numerical model is realized using technologies CUDA and GPUDirect for hybrid computational systems (supercomputers) with graphic processors (CPU–multi-GPU) [16].

1. Mathematical model of the vibrationally-excited gas

We will consider dynamics of the non-equilibrium vibrationally-excited gas, which in a two-dimensional region (x, y) is characterized by a flow velocity $\mathbf{u} = \{u, v\}$, a density ϱ, a pressure p, a static T and a vibrational T_V temperature. In the non-equilibrium vibrationally-excited gas $T_V > T$. The dynamics of the non-equilibrium gas taking into account viscosity, thermal conductivity, vibrationally-translational relaxation (VT-relaxation), heating and cooling will be described by the following conservative system of equations of fluid dynamics [4,10,11]:

$$\frac{\partial \mathbf{U}}{\partial t} + \frac{\partial \mathbf{F}}{\partial x} + \frac{\partial \mathbf{G}}{\partial y} = \mathbf{\Phi}, \tag{1}$$

where

$$\mathbf{U} = \begin{pmatrix} \varrho \\ \varrho u \\ \varrho v \\ E \\ \varrho \varepsilon_V \end{pmatrix}, \quad \mathbf{F} = \begin{pmatrix} \varrho u \\ \varrho u^2 + p - \sigma_{xx} \\ \varrho uv - \sigma_{xy} \\ (E+p)u - \varkappa \nabla_x T - u\sigma_{xx} - v\sigma_{xy} \\ \varrho \varepsilon_V u \end{pmatrix},$$

$$\mathbf{G} = \begin{pmatrix} \varrho v \\ \varrho uv - \sigma_{xy} \\ \varrho v^2 + p - \sigma_{yy} \\ (E+p)v - \varkappa \nabla_y T - v\sigma_{yy} - u\sigma_{xy} \\ \varrho \varepsilon_V v \end{pmatrix}, \quad \mathbf{\Phi} = \varrho \begin{pmatrix} 0 \\ 0 \\ 0 \\ -\dot{\varepsilon}_V \\ \dot{\varepsilon}_V \end{pmatrix},$$

$E = \varrho\left(0.5|\mathbf{v}|^2 + \varepsilon\right)$, ε is a specific internal energy (translational and rotational degrees of freedom), ε_V is a specific vibrational energy, σ_{xx}, σ_{xy}, σ_{yy} are components of a viscous stress tensor, $\varkappa$ is a thermal conductivity coefficient, $\nabla = \{\nabla_x, \nabla_y\} = \left\{\frac{\partial}{\partial x}, \frac{\partial}{\partial y}\right\}$, $\dot{\varepsilon}_V$ is a specific power of vibrationally-translational energy exchange, which is calculated using the Landau–Teller formula: $\dot{\varepsilon}_V = (\varepsilon_V^e - \varepsilon_V)/\tau$, where $\varepsilon_V^e \equiv \varepsilon_V(T)$ is a specific vibrational energy in an equilibrium state when $T_V = T$, τ is a time of vibrational relaxation. The specific vibrational energy of the gas ε_V, which depends on the respective vibrational temperature T_V, will be written as follows [4,10,11]:

$$\varepsilon_V(T_V) = \frac{\mathscr{R}}{M}\sum_{\ell=1}^{N_V}\frac{r_\ell\theta_\ell}{\exp(\theta_\ell/T_V) - 1},$$

where N_V is a number of vibrational modes, θ_ℓ is a typical vibrational temperature of the ℓ-the mode, r_ℓ is a degeneracy degree of the ℓ-mode.

The time of vibrational relaxation will be generalized as follows [10,11]:

$$\tau = \frac{p_A T^n}{p}\,\frac{\exp\left\{a_0 + a_1 T^{-1/3} + a_2 T^{-2/3} + a_3 T^{1/3}\right\}}{1 - m\exp(-\theta_*/T)},$$

where p_A is an atmospheric pressure, θ_* is a minimum one the typical temperatures of the vibrational modes [17], calibration coefficients of the relaxation model area_i, n and m [4,10,11,17].

The system of equations (1) is closed by the equation of state for the ideal gas: $p = \mathscr{R}\varrho T/M$, $\varepsilon = p/[(\gamma - 1)\varrho]$, where M and γ are a molar mass and an adiabatic index of the gas, $\mathscr{R}$ is an universal gas constant.

2. Numerical method and the parallel algorithm

The numerical solution of the system of equations (1) is based on the method MUSCL [10,11,15]. After discretization of continuous magnitudes $\mathbf{U}(x, y, t)$ in nodes of a space time grid: $\mathbf{U}(x, y, t) \to \mathbf{U}(x_i, y_j, t_n) \equiv \mathbf{U}_{i,j}^n$, where $t_{n+1} = t_n + \Delta t_n$ ($n = 0, 1, \ldots$ is a time layer), Δt is a time step, $x_{i+1} = x_i + \Delta x$ ($i = 0, \ldots, N_x + 4$), $y_{j+1} = y_j + \Delta y$ ($j = 0, \ldots, N_y + 4$), $\Delta x = L_x/N_x$ and $\Delta y = L_y/N_y$ are sizes of spatial cells, L_x and L_y are sizes of the computation region, N_x and N_y are a number of computation cells by the x- and y-coordinates, respectively. The numerical algorithm of the method MUSCL will be written as

$$\mathbf{U}_{i,j}^{n+1} = \mathbf{U}_{i,j}^n + \Delta t_n\left(\frac{\hat{\mathbf{F}}_{i-1/2,j} - \hat{\mathbf{F}}_{i+1/2,j}}{\Delta x} + \frac{\hat{\mathbf{G}}_{i,j-1/2} - \hat{\mathbf{G}}_{i,j+1/2}}{\Delta y} + \hat{\mathbf{\Phi}}_{i,j}\right), \qquad (2)$$

where fractional indices $i \pm 1/2$ and $j \pm 1/2$ correspond to boundaries of cells of the computation grid ($x_{i\pm1/2} = x_i \pm \Delta x/2$, $y_{j\pm1/2} = y_j \pm \Delta y/2$), $\hat{\mathbf{F}}_{i\pm1/2,j} = \frac{1}{\Delta t_n}\int\limits_{t_n}^{t_{n+1}}\mathbf{F}_{i\pm1/2,j}(t)dt$, $\hat{\mathbf{G}}_{i,j\pm1/2} = \frac{1}{\Delta t_n}\int\limits_{t_n}^{t_{n+1}}\mathbf{G}_{i,j\pm1/2}(t)dt$, $\hat{\mathbf{\Phi}}_{i,j} = \frac{1}{\Delta t_n}\int\limits_{t_n}^{t_{n+1}}\mathbf{\Phi}_{i,j}(t)dt$. At each moment of time, values of the gas-dynamic fluxes $\hat{\mathbf{F}}_{i\pm1/2,j}$ and $\hat{\mathbf{G}}_{i,j\pm1/2}$ are calculated at boundaries of the computation cells using approximate Riemann solvers HLL/HLLC [18]. The second order of accuracy in the method MUSCL is achieved by using a predictor-corrector algorithm for time advancement and piecewise linear reconstruction of grid functions using TVD-limiters (Total Variation Diminishing) [15].

In order to increase performance of numerical modeling of the supersonic gas-dynamic flows on the computation cells with tens and hundreds of millions cells, our algorithm of the method MUSCL (2) was paralleled using the technologies OpenMP-CUDA and GPUDirect that are used in hybrid computational systems with several graphic processors (CPU–multi-GPUs). Using GPUDirect makes it possible to provide fast direct data exchange between the GPUs avoiding CPU due to an interface NVLINK [14,16,19]. The implemented parallel algorithm OpenMP–CUDA for the computational systems CPU–multi-GPUs makes it possible to accelerate calculations in 100–1000 times as compared to parallel versions of the code for CPU [19].

3. Results of numerical modeling

In the numerical model (2), we transit to dimensionless magnitudes: $\bar{f} = f/l_f$, where l_f is a typical scale of the magnitude f. Typical scales of the numerical models according to the studies [10,11,19] are: $l_t = \tau_0$, $l_u = c_0$, $l_{xy} = c_0\tau_0$, $l_T = T_0$, $l_p = p_0$, $l_\varrho = \varrho_0/\gamma$, where a lower index $\ll 0 \gg$ corresponds to initial spatially-homogeneous distributions of the gas and $c_0 = \sqrt{\gamma p_0/\varrho_0}$ is a speed of sound.

Investigation of nonlinear dynamics of the gas-dynamic instabilities in the non-equilibrium gas (see the studies [10–12,19]) requires using high spatial resolution in the numerical models, which is determined by an optimal value of the step of the computation cell: $\Delta\bar{x} = \Delta\bar{y} = 0.01$.

Let us consider a model problem on outflow of the supersonic jet of the non-equilibrium vibrationally-excited gas ($\bar{T}^{(jet)} = 0.3$, $\bar{T}_V^{(jet)} = 3$, $\bar{p}^{(jet)} = 1$, $\bar{u}^{(jet)} = 2$) into the flat channel with the equilibrium gas at rest ($\bar{T}^{(ch)} = \bar{T}_V^{(ch)} = 0.3$, $\bar{p}^{(ch)} = 1$, $\bar{u}^{(ch)} = 0$). The jet inflows at a left boundary of the computation region with the Mach number $M \approx 3.65$, while at a right boundary free-flow conditions are pre-defined. At the cooled channel walls (an upper and a lower boundary of the computation region), „solid wall“ conditions are pre-defined (sticking non-flowing) and a constant surface temperature $\bar{T}_{ex} = 0.3$ is maintained. Values of the dimensionless parameters of the mathematical model are selected

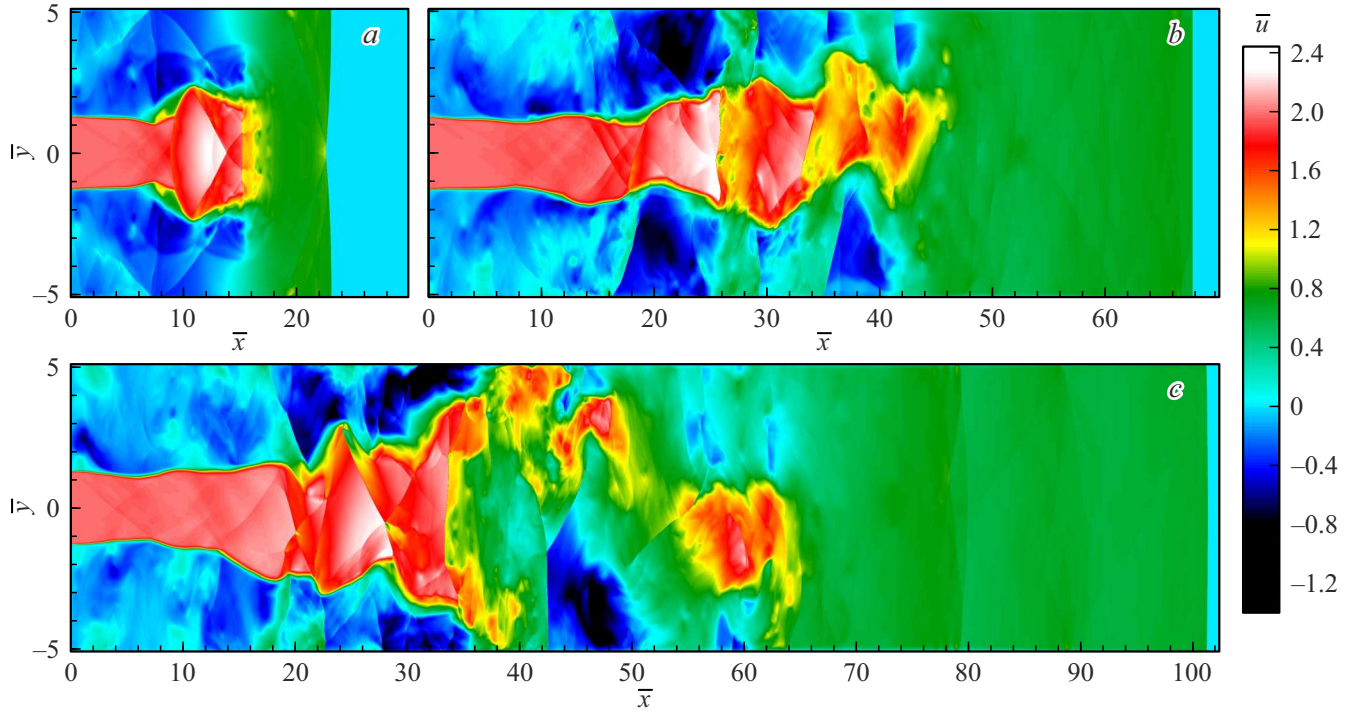

Figure 1. Evolution of the shock-wave structure of the flow in a flat channel when injecting the non-equilibrium vibrationally-excited gas jet. Distributions of the velocity $\bar{u}$ are shown at various times: a — $\bar{t} = 20$; b — $\bar{t} = 60$; c — $\bar{t} = 90$.

according to basic models [10,11,19]: $\gamma = 1.4$, $\bar{a}_1 = 10$, $\bar{a}_2 = \bar{a}_3 = n = m = 0$, $\bar{\theta}_* = \bar{\theta}_1 = 6$. The channel sizes are $\bar{L}_x = 102.4$ and $\bar{L}_y = 10.24$ and the respective number of the computation cells is $N_x = 1024$ and $N_y = 10240$. The total number of the computation cells is $N = 10\,485\,760$. A cross size of the jet is $\bar{D}_y^{(jet)} = 2.56$ or $N_y^{(jet)} = 256$. The supersonic jet is injected along a middle line of the channel with a slight downshift by the magnitude $\Delta\bar{y}$, which is required for evolution of unstable bending modes of the jet.

Fig. 1 shows dynamics of progress of the shock-wave structures in the flat channel during outflow of the supersonic jet of the non-equilibrium gas. The initial stage of evolution (Fig. 1, a) first included formation of the shockwave related to supersonic outflow of the gas into the stationary medium. Then, behind the front of the this shockwave a jet outflow area forms the shock-wave structures that are induced by progress of the unstable modes of the jet (of Kelvin-Helmholtz ones and reflective acoustic harmonics). At the same time, intensity of these shock-wave structures in the non-equilibrium jet turns out to be higher than in the non-equilibrium jet [19]. It is related to acoustic activity of the non-equilibrium vibrationally-excited gas, which results in evolution of acoustic instability [10–12,19]. During further evolution (Fig. 1, b, c), along with symmetric (pinch) modes of the jet, instability of antisymmetric (bending) modes of the jet also evolves and results in bending of the jet flow and destruction of the jet in the range $\bar{x} > 50$. At the nonlinear stage of evolution the unstable modes of the jet form a complex shock-wave system in the channel.

The shock-wave and vortical flow structure at the time $\bar{t} = 90$ is shown in detail in Fig. 2. The complex system of shockwaves and vortices can be conveniently analyzed in shading maps of distribution of the gas-dynamic magnitudes (Fig. 2, a), which allow selecting flow heterogeneities by visualizing gradients of these magnitudes (similar to the schlieren method in physical experiments). By distribution of the static ($\bar{T}$) and the vibrational ($\bar{T}_V$) temperature in Fig. 2, b, c, the vortex structures and the oblique shockwaves (only for $\bar{T}$) are well selected. Along with higher intensity of the shock-wave and vortical structures, the non-equilibrium jet flows are also characterized by significant gas heating in the jet destruction area ($35 < \bar{x} < 65$), which is caused by transfer of vibrational energy into thermal one behind the shockwave front and in the zone of intense vortex flows. As it is seen in Fig. 2, b, c, in the range ($\bar{x} > 70$) the gas flow is almost an equilibrium one $\bar{T}_V \sim \bar{T}$.

Performance of the computational code can be conveniently analyzed by means of time of processing a single computation cell in the numerical algorithm t_{cell}. In our parallel realization OpenMP–CUDA–GPUDirect of the computational code for GPUs this time for N=10 485 760 is: $t_{cell}^{(1GPU)}$=1.8 ns, $t_{cell}^{(2GPU)}$=0.95 ns, $t_{cell}^{(4GPU)} = 0.49$ ns, $t_{cell}^{(8GPU)} = 0.27$ ns. The best time of processing the single computation cell in the parallel OpenMP version of the code for CPUs (40 cores) is $t_{cell}^{(CPU)} = 325$ ns.

Let us note that our parallel code OpenMP–CUDA–GPUDirect can be scaled for modeling the more complex three-dimensional flows of the non-equilibrium gas. At the

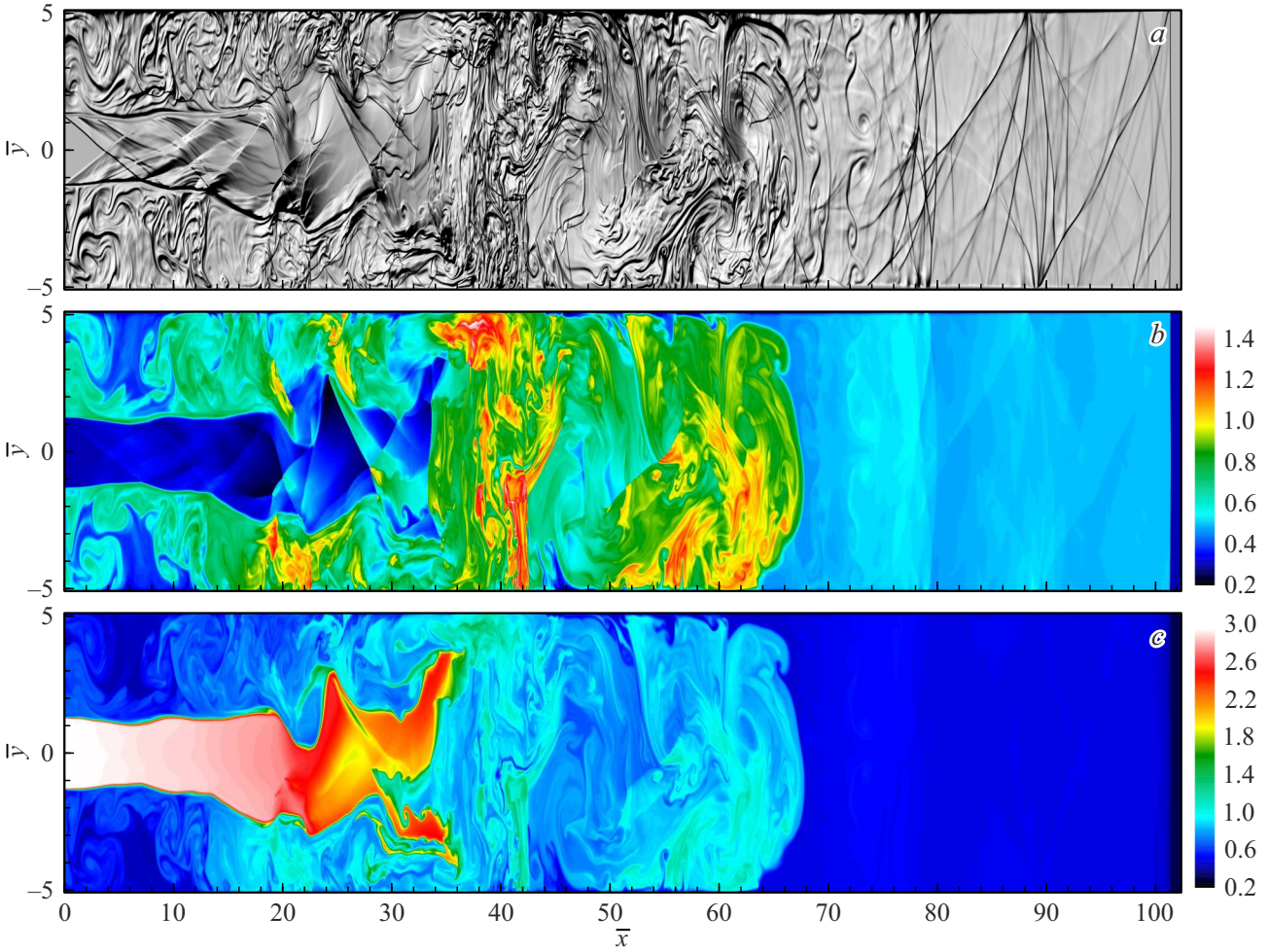

Figure 2. Flow structure (vortical and shock-wave) in the flat channel when injecting the non-equilibrium vibrationally-excited gas jet. The following distributions are shown at the time $\bar{t} = 90$: *a* — of the density $\bar{\varrho}$ (a shading representation); *b* — of the temperature $\bar{T}$; *c* — of the vibrational temperature $\bar{T}_V$.

same time, our estimates show that the time of processing the single computation cell will increase in 1.5−1.7 times due to appearance of an additional equation for the z-component of the velocity as well as additional calculations of inclinations during piecewise linear reconstruction of the grid functions and fluxes of conservative magnitudes $\mathbf{U}$ along the z-direction. In the two-dimensional version of the code, a capacity of the required GPU memory is ~ 240 bytes per one computation cell, while a transition into three-dimensional implementation will required ~ 384 bytes per cell.

Conclusions

Based on the numerical gas-dynamic method MUSCL, the parallel version OpenMP–CUDA–GPUDirect of the computational code is realized for modeling the two-dimensional supersonic flows of the non-equilibrium vibrationally-excited gas with various models of the time of VT-relaxation on the hybrid supercomputers with the graphic processors (CPU–multi-GPU). The study has used the supercomputers NVIDIA DGX-1 (VolSU) and Lomonosov 2 (Volta 1,2 — MSU) with the graphic processors NVIDIA V100. The transition into the parallel version of the code for GPUs made it possible to accelerate the calculations in 180−1200 times as compared to the parallel code for CPUs.

The designed parallel algorithm of the method MUSCL was tested on the two-dimensional problem of numerical modeling of dynamics of the supersonic flows of the non-equilibrium vibrationally-excited gas in the flat channel. It is shown that during outflow of the non-equilibrium supersonic jet into the equilibrium gas at rest, a complex shock-wave and vortical structure is formed in the channel, whose intensity turns out to be higher as compared to the case of injection of the equilibrium jets. Besides, due to evolution of gas-dynamic instabilities of the pinch and bending modes, the gas is significantly heated as a result of transfer of vibrational energy into thermal one by intense relaxation processes.

The results of numerical modeling of dynamics of the supersonic flows of the non-equilibrium vibrationally-excited

gas, which are obtained in the study, and the shock-wave and vortical structures detected in the numerical models can be useful when designing new types of detonation jet engines and gas-dynamic lasers [7] as well as experimental energy installations for generating powerful shock-wave pulses [20].

Funding

This work supported by the Russian Science Foundation (grant no. 23-71-00016, https://rscf.ru/project/23-71-00016/). The research is carried out using the equipment of the shared research facilities of HPC computing resources at Lomonosov Moscow State University.

Conflict of interest

The authors declare that they have no conflict of interest.

References

[1] F.A. Maksimov. Fiziko-khimicheskaya kinetika v gazovoi dinamike, **26** (1), 1160 (2025) (in Russian). http://chemphys.edu.ru/issues/2025-26-1/articles/1160/
[2] R. Seleznev. Fluid Dynamics, **58**, 1584 (2023). DOI: 10.1134/S0015462823602607
[3] I.A. Shirokov, T.G. Elizarova. Fiziko-khimicheskaya kinetika v gazovoi dinamike, **26** (1), 1173 (2025) (in Russian). http://chemphys.edu.ru/issues/2025-26-1/articles/1173/
[4] S.T. Surzhikov. Fluid Dynamics, **58** (1), 113 (2023). DOI: 10.1134/S0015462822700033
[5] A.I. Osipov, A.V. Uvarov. UFN, **162** (11), 1 (1992) (in Russian). DOI: 10.3367/UFNr.0162.199211a.0001
[6] G.G. Antonov, V.B. Kovshechnikov, F.G. Rutberg. ZhTF, **86** (5), 96 (2016) (in Russian).
[7] A.V. Avdeed, A.S. Boreisho, I.A. Kiselev, A.V. Morozov, A.E. Orlov. Fotonika, **14** (8), 648 (2020) (in Russian). DOI: 10.22184/1993-7296.FRos.2020.14.8.648.661
[8] A.I. Osipov, A.V. Uvarov. UFN, **166** (6), 639 (1996) (in Russian).
[9] V.G. Makaryan, N.E. Molevich. Plasma Sources Sci. Technol., **16** (1), 124 (2007). DOI: 10.1088/0963-0252/16/1/017
[10] S.S. Khrapov. Fluid Dynamics, **59** (4), 899 (2024). DOI: 10.1134/S0015462824602584
[11] S.S. Khrapov. Fiziko-khimicheskaya kinetika v gazovoi dinamike, **25** (7), 1151 (2024) (in Russian). http://chemphys.edu.ru/issues/2024-25-7/articles/1151/
[12] S.S. Khrapov, G.S. Ivanchenko, V.P. Radchenko, A.V. Titov. ZhTF, **93** (12), 1727 (2023) (in Russian). DOI: 10.61011/JTF.2023.12.56805.f213-23
[13] J. McKevitt, E.I. Vorobyov, I. Kulikov. J. Parallel Distributed Computing, **195**, 104977 (2025). DOI: 10.1016/j.jpdc.2024.104977
[14] A. Radhakrishnan, H. Le Berre, B. Wilfong, J.-S. Spratt, M. Rodriguez, T. Colonius, S.H. Bryngelson. Comp. Phys. Commun., **302**, 109238 (2024). DOI: 10.1016/j.cpc.2024.109238
[15] B. van Leer, J. Comp. Phys., **32** (1), 101 (1979).
[16] S.S. Khrapov, A.V. Khoperskov. Supercomp. Frontiers and Innovations, **11** (3), 27 (2024). DOI: 10.14529/jsfi240302
[17] E.A. Kovach, S.A. Losev, A.L. Sergievskaya, N.A. Khrapak. Fiziko-khimicheskaya kinetika v gazovoi dinamike, **10**, 332 (2010) (in Russian). http://chemphys.edu.ru/issues/2010-10/articles/332/
[18] E.F. Toro, M. Spruce, W. Speares. Shock Waves, **4** (1), 25 (1994).
[19] S. Khrapov. Matematicheskaya fizika i komp'yuternoe modelirovanie, **28** (1), 60 (2025) (in Russian). DOI: 10.15688/mpcm.jvolsu.2025.1.5
[20] V. Radchenko, S. Khrapov, A. Khoperskov. in *2024 6th International Conference on Control Systems, Mathematical Modeling, Automation and Energy Efficiency (SUMMA)*. IEEE Xplore (Lipetsk, Russian Federation, 2024), p. 533. DOI: 10.1109/SUMMA64428.2024.10803831

Translated by M.Shevelev